REVUE DE

PALÉOBIOLOGIE

VOLUME 38 (2) – 2019

muséum Genève

Une institution
Ville de Genève

www.museum-geneve.ch

VILLE DE GENÈVE

Revue de Paléobiologie, *Genève* (décembre 2019) 38 (2): 535-551 ISSN 0253-6730

Biostratigraphic analysis of *Assilina* and calcareous nannofossil assemblages from the lower part of the Jahrum Formation (Zagros zone, Iran): insight into systematic of *Assilina* d'Orbigny

Mehdi Hadi[1*], Mohammad Parandavar[1, 2], Majid Mirzaie-Ataabadi[3] & Azam Zareh[4]

[1] *Department of Geology, Faculty of Science, Ferdowsi University of Mashhad, Mashhad, Iran. E-mail: mehdi_hadi_s@yahoo.com, E-mail: parandavar.m@mail.um.ac.ir*
[2] *National Iranian Oil Company, Exploration Directorate, Sheikh Bahaei Square, Tehran, Iran.*
[3] *Department of Geology, Faculty of Sciences, University of Zanjan, Zanjan, Iran. E-mail: majid.mirzaie@znu.ac.ir*
[4] *Department of Geology, Payame Noor University, Shiraz, Iran. E-mail: zare.geologist@gmail.com*
* *Corresponding autor*

Abstract
The present research is a study on the *Assilina* assemblages which are recorded from the lower part of the Jarum Formation in the Buldaji section, exposed in the Zagros region, southwest Iran. Studies on the systematic analysis and biostratigraphy of these assemblages resulted in diagnosis of three *Assilina* taxa: *A.* ex. interc. *cuvillieri* Schaub, 1981-*tenuimarginata* Heim, 1908, *A. aspera* Doncieux, 1948, and *A.* aff. *aspera* (Doncieux, 1948), associated with calcareous nannofossil assemblage. Biostratigraphically, we present new data assignable the SBZ13 and NP15/ CNE9-10 zones from the lower part of the Jahrum Formation (Zagros region) pertaining to the central Tethys. This integrated study indicates a precise correlation between *Assilina* and calcareous nannofossils zonations of the studied interval at a local stratigraphical scale, enabling us to make possible projections for future stratigraphic studies in the vicinity of Tethyan regions.

Keywords
Assilina, Calcareous nannofossils, Jahrum Formation, Shallow Benthic Zone (S.B.Z.).

1. INTRODUCTION

Assilina are among the common larger benthic foraminifera (L.B.F.) in the Eocene shallow-marine deposits of Iran, even though they have been poorly studied so far. This paper is the first attempt on the study of *Assilina* systematics, almost four decades after the latest taxonomic studies carried out by Rahaghi (1978, 1980), Rahaghi & Schaub (1976), and Mojab (1982) on some *Assilina* species from different parts of Iran. Although, numerous studies have focused on the biostratigraphy and paleoecology of the early Paleogene shallow marine successions in the Zagros basin (i.e. The Jahrum, Shahbazan, and Tale-Zang Formations), detailed taxonomic studies on the LBF have not been correctly carried out (e.g. Maghfouri-Moghadam & Taherpour-Khalil-Abad, 2012; Izadighalati & Ahmadi, 2017; Almasinia, 2017; Amirshahkarami & Zebarjadi, 2018). In other words, the only recent study with focus on the internal morphology of porcelaneous foraminifera from the Jahrum Formation has been presented by Hottinger (2007). On contrary, the nummulitid fauna of the Eocene shallow-water carbonate platforms of the western Tethyan have been studied over the last fifty years and illustrated in monographs and papers (e.g. Schaub, 1981; Boukhary, 1988; Boukhary *et al.,* 1995), and afterward applied for designating the shallow benthic zones (SBZ) by Serra-Kiel *et al.* (1998). Hence, this zonation is used in numerous articles published so far. Recently, these biozones are correlated based upon the systematics and biostratigraphic interpretation of the LBF in central and eastern Tethyan regions (e.g. Zhang *et al.,* 2013; Ben Ismail-Lattrache *et al.,* 2014; Ahmad *et al.,* 2015; Ozcan *et al.,* 2015, 2016, 2018, Hadi & Vahidinia, 2019; Hadi *et al.,* 2019a-c). In fact, LBF assemblages from Eocene successions of Iran and within the central Tethys still not studied in detail. Furthermore, the LBF are required to be associated with the planktonic microfossils group, such as calcareous nannofossils for better biostratigraphic analysis.

Submitted October 2018, accepted July 2019
Editorial handling: A. Piuz
DOI: 10.5281/zenodo.3579357

So far, several Paleogene calcareous nannofossil biozonation schemes were established for low to high latitude regions, which includes Martini (1971; N.P. zones), Okada & Bukry (1980; C.P. zones), and Varol (1989; N.N.T. zones). Agnini *et al.* (2014) have revised the previous calcareous nannofossil biozonation frameworks and established the new Paleogene scheme (C.N.P. / C.N.E. / C.N.O. zones) for the low to middle latitudes sites. In the past decades, the standard biozonations of Martini (1971), and Okada & Bukry (1980) have been correlated with the planktonic-benthic foraminifera, and magneto-geochronological scales (Berggren *et al.,* 1995, Berggren & Pearson, 2005; Serra-Kiel *et al.,* 1998). While this correlation is related to the western parts of the Tethyan realm, no accurate data from Iran is still available on the position of the LBF, like the genus *Assilina*, in the global time scale.

Hence, our main objective is to review the *Assilina* systematics in the lower parts of the Jahrum Formation and to integrate the LBF and calcareous nannofossils biozones, which are correlated with the SBZ zones after Serra-Kiel *et al.* (1998). When the preceding researches in the studied region of the Jahrum Formation are investigated it is seen that these are chiefly studies about sedimentology fields (Vaziri-Moghaddam *et al.,* 2002; Khatibi-Mehr *et al.,* 2012; Almasinia, 2017), while the only noteworthy paleontological study with detailed taxonomy on the *Assilina* assemblage was conducted by Mojab (1982). Our work is pioneer in study of *Assilina* distribution in the frame of correlation between the SBZ and nannofossil biozones in Iran. This integrated study can provide valuable data pertaining to the age and knowing of the relationship between the distribution range of *Assilina* and nannofossil faunas in the west (Europe and Mediterranean) and central (Iran) Tethys within the global framework. However, for a better understanding of the parameters controlling of *Assilina* distribution across the globe, we need a reconstruction of the sedimentary conditions that is beyond the scope of this work.

2. GEOLOGICAL SETTING, MATERIAL, AND METHODS

The Iranian plateau is part of the large mountain belt of the Alpine-Himalayan system, which has been subdivided into nine sedimentary-structural provinces (e.g. Stöcklin, 1968; Shafaii Moghadam & Stern, 2014; Fig. 1a). These provinces from North to South are: (1) Kopeh-Dagh Zone in NE Iran; (2) The southern Caspian Sea Basin; (3) Alborz zone in N-NW Iran; (4) The Central Iranian block or Cimmeria, consisting of three major old continental blocks (from E to W: Lut, Tabas, and Yazd), separated by major faults (e.g. Alavi, 1991); (5) Eastern Iranian suture Zone; (6) Urumieh-Dokhtar (Sahand–Bazman) magmatic arc, (7) Zagros Zone, (8) Sanandaj–Sirjan Zone, and (9) Makran Zone (Fig. 1a). The Zagros Zone is one of the most important geological regions in middle parts of the Alpine-Himalayan belt in Iran. It extends from the southeastern Turkey through northern Syria and Iraq to southwest Iran (Alavi, 2004). According to Motiei (1993), the Zagros mountains are mainly divided into: (1) the simply folded Zagros, (2) the imbricate thrust zone, and (3) the Khuzestan Plain. In general, the Zagros Basin is the result of the collision between the continental Afro-Arabian and the so-called Iranian block during the late Cretaceous and later times (e.g. Alavi, 2004). Therefore, this basin was part of the stable Gondwana supercontinent during the Paleozoic. Afterward, it becomes a passive margin and convergent orogeny in the Mesozoic and Cenozoic eras, respectively (Motiei, 1993; Bahroudi & Koyi, 2004; Heydari, 2008). Likewise, the sedimentary column of the Zagros Basin is composed of the Cambrian to Plio-Quaternary deposits, which reaches to 8-10 km (Alavi, 2004; Sherkati & Letouzey, 2004). While, the Eocene shallow-marine successions are represented by different Formations, such as Shahbazan, Taleh-Zang and Jahrum Formations within the Zagros zone (Fig. 1b-c). Our studies in south of Esfahan region (Zagros zone) are concentrated on the *Assilina* bearing horizons of the Eocene carbonate deposits of the Jahrum Formation (Buldaji section).

The type section of Jahrum Formation with a total thickness of 467.5 m was described from shallow water carbonates of the Paleocene to Late Eocene sedimentary successions at Kuh-e Jahrum in south of Jahrum town, and is about 200 km southeast of Shiraz city by James & Wynd (1965). At the type locality, the Jahrum Formation conformably overlies upper Cretaceous to Early Eocene beds of silty marl, dolomites and evaporates belonging to the Sachun Formation. In some places, where the Sachun Formation is absent, the Jahrum Formation overlies carbonates of the Tarbur, red beds of the Kashgan and also, shales of the Gurpi Formations (Motiei, 1993). There is the Jahrum Formation overlain by an unconformable erosion sedimentary surface of the Asmari Formation (Oligocene-Miocene) (Motiei, 1993).

The Eocene carbonates sedimentary in the Buldaji section are represented by the Jahrum Formation (coordinates: 51° 00' 08" longitude; 31° 56' 33" latitude), which is located 5 km west of Buldaji town along Hamzeh-Ali road near to the Kalbibak village, which is about 55 km west of Boroujen city (Fig. 1d). This section is situated about 150 km southwest of Esfahan city (Fig. 1d). The Buldaji section is substantially composed of limestone, marl and clayey limestone with thickness of 160 m, and the lower boundary is conformable in which the Jahrum Formation gradually develops from the Pabdeh Formation. The top of the section is covered by alluvium. According to Almasinia (2017), the results of microfacies and biostratigraphic data are indicative of depositions in a distally steepened ramp with abundance of planktonic and benthonic foraminiferal assemblages during the

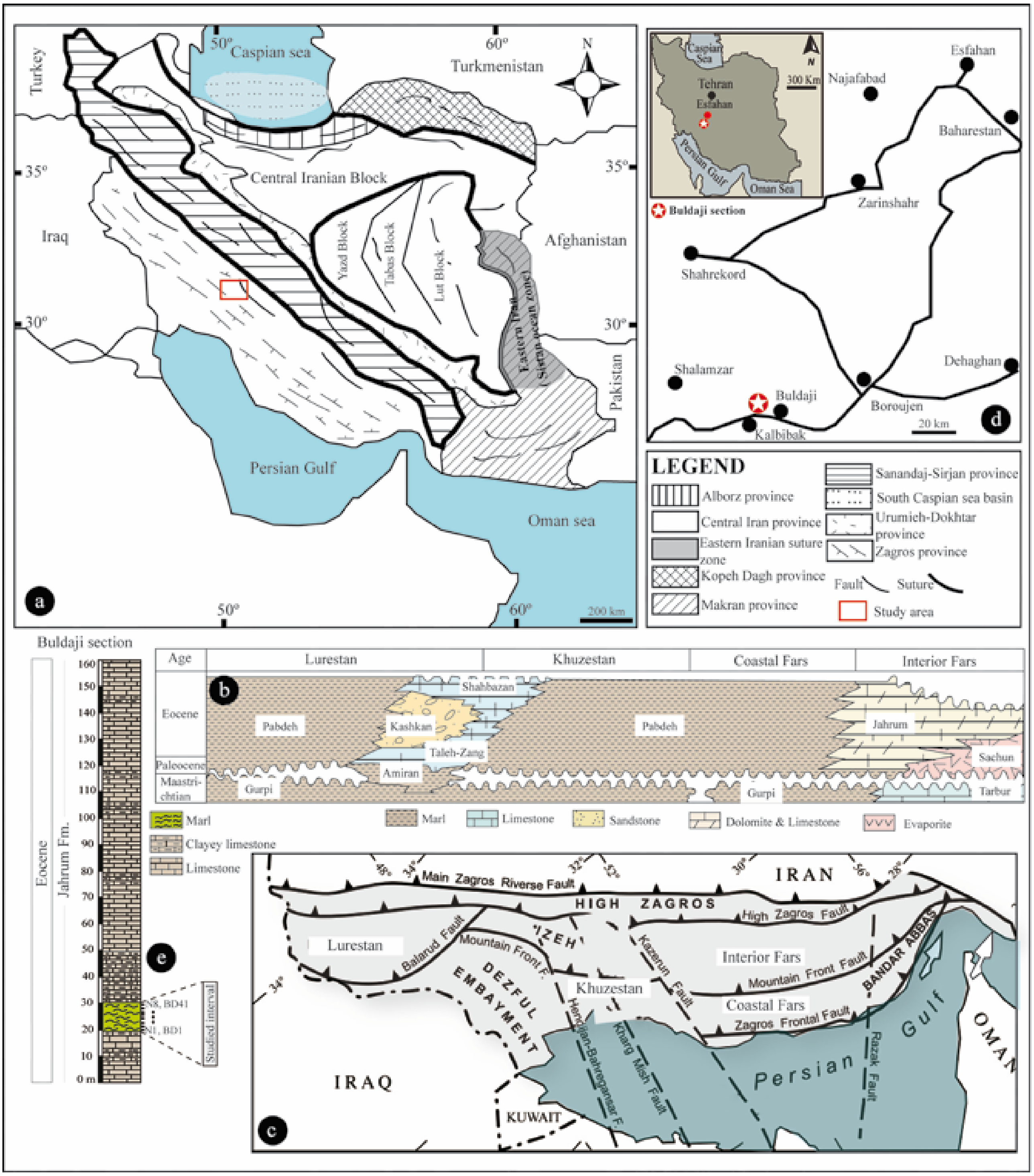

Fig. 1: **(a)** General map of Iran showing the nine geologic provinces (adapted from Stöcklin, 1968 and Shafaii Moghadam & Stern, 2014). **(b)** Correlation chart of the Masstrichtian-early Paleogene deposits for the Zagros Basin of southwest Iran (modified from Ala, 1982). **(c)** Main structural subdivisions of the Zagros fold and thrust belt (adapted from Sherkaty & Letouzey, 2004). **(d)** Location map showing the position of the Buldaji section. **(e)** Generalized stratigraphic column of the Buldaji section (Jahrum Fm.) in the Zagros region, SW Iran and the studied interval.

late Cuisian (SBZ12) to early Lutetian (SBZ13) in the Buldaji section (=Hamzeh-Ali section), while the estimated age based upon the biostratigraphic range of LBF was not in accordance with the strontium isotope dating. However, she noted that the deposits of the Buldaji (=Hamzeh-Ali section) succession belongs to the late Cuisian-early Lutetian age based on foraminiferal taxa identified, but the taxonomic identifications are not reliable, only on the basis of random thin-sections without providing the axial and equatorial sections of isolated LBF. Moreover, Khatibi-Mehr *et al.* (2012) proposed six 3rd order sequences that were analyzed by the interpretations of field observation and variation on vertical facies, where the sequence boundaries are type-2, as well as transgressive systems tracts with lamellar-perforate LBF are present in marls, marly limestone and limestones in the Boldaji section. Assemblages of LBF with high abundance and diversity as major elements of biogenic components in the Jahrum Formation are mainly composed of alveolinids, nummulitids, orthophragminids and conical foraminifera.

The *Assilina* species presented here are found within marly layers with thickness of 10 m in the lower part of the Buldaji section (Fig. 1e). A total 41 free-specimens (samples BD1-BD41) were collected and selected for the biometric and taxonomic studies. The species of *Assilina* were chiefly determined according to the taxonomic descriptions given after Doncieux (1948), Schaub (1981), Mojab (1982), and Sirel & Deveciler (2018). The thin sections (2.5 cm × 7.5 cm) were digitally photographed under transmitted-light (Olympus BX51). The occurrences of *Assilina* were identified in thin-sections according to the shallow benthic zones proposed by Serra-Kiel *et al.* (1998). The material used in this work is housed in the collection of M. Hadi at Ferdowsi University of Mashhad (F.U.M.).

For calcareous nannofossils analysis, eight samples (samples n1-n8) were prepared in the simple smear slides (described by Bown & Young, 1998; Parandavar & Hadavi, 2019), using standard light microscope (Olympus BX53) in parallel-polarised (P.P.L.) and cross-polarised (X.P.L.) light by adding the quartz (Q.P.) and gypsum (G.P.) plate at a magnification of 1250-2000x. The studies of Romein (1979), Perch-Nielsen (1985), Aubry (1984, 1989), Bown (2005), Farinacci & Howe (2016) are used for calcareous nannofossil taxonomy in the present study. In order to assign biozones to the samples and for age determination, the low-latitude zonation schemes of Martini (1971; NP zones) and Agnini *et al.* (2014; CNE zones) were followed.

3. RESULTS

3.1. Systematic Palaeontology

Family Nummulitidae Blainville, 1827
Genus *Assilina* d'Orbigny, 1839
Type species: *Assilina depressa* d'Orbigny, 1839

***Assilina* ex. interc. *cuvillieri* Schaub, 1981-*tenuimarginata* Heim, 1908**
Figs 2a-l & 3a-h

1981. *Assilina cuvillieri* Schaub, p. 210, pl. 88, figs 22-26 (non); pl. 89, figs 1-49.
2003. *Assilina cuvillieri* Schaub.– Pavlovec, pl. 1, figs 3, 4.
2014. *Assilina cuvillieri* Schaub.– Deveciler, lev. 15, şek. 24-50; lev. 16, şek. 1-6.
2018. *Assilina cuvillieri* Schaub.– Sirel & Deveciler, pl. 44, figs 1-12.

Number of specimens examined: 25

Description: The megalospheric generation has a lenticular to slightly inflated lenticular form with diameter from 7.1 mm to 8.3 mm and thickness from 1.2 mm to 1.6 mm. The granules are fine, and mostly concentrated on the polar area as well as arranged on and in-between the radial to slightly curved septal filaments towards the margin. The steps of coiling are from tight to lax, so that the spire openings are regular and showing an increase gradually towards the last whorl. The chambers are higher than long and length of the chambers increases from the first whorl to the last one with the marginal cord relatively thick and regular. The septa are straight in the inner whorls, and then become inclined sometimes towards in the outer whorls. Number of whorls per radius is: 3 whorls in a radius of 1.4-1.6 mm, 5 whorls in a radius of 2.4-3 mm, and 7 whorls in a radius of 3.1-3.9 mm. The proloculus has diameter ranges of 390-470 µm (Tabl. 1). The microspheric generation has an inflated lenticular, and biumbonate test with slightly narrow and pointed margin, especially in juvenile forms. The diameter ranges between 11 and 17.8 mm and thickness ranges between 1.6 mm and 3 mm. The granules are remarkably dense at the central area and arranged on the swelling part, which is surrounding the central depression, they are less visible in the adult forms. In addition, they are arranged from the centre to the periphery on the radial septal filaments and sometimes scattered rarely between them. The rate of spire openings increase gradually from the first whorl to the last one, whilst they show a sudden increase in the outer whorls. The chambers are somewhat subrectangular and higher than long with ratio of approximately 1.5-2 times. The marginal cord is fairly thick, and the average thickness is almost constant at all over growth stages. The septa are straight in the inner and middle whorls, and occasionally become slightly inclined in the outer whorls. Number of whorls per radius: 11

Table 1: Key features data of *Assilina* populations from the Buldaji section.

Megalospheric form (A-form)

Characters	*Assilina aspera*	*Assilina* aff. *aspera*	*Assilina* ex. interc. *cuvillieri-tenuimarginata*
Diameter (mm) Thickness (mm)	6.7-7.7 1.8-2	4.7-5.1 1.8-2.1	7.1-8.3 1.2-1.6
Rate of spire opening	1, 1.1, 1.3, 1.6, 1.8, 2.1,2.2	1, 1.2, 1.3, 1.7, 1.8	1, 1.1, 1.3, 1.4, 1.7, 1.5
Number of whorls per radius per mm	3 whorls 1-1.26 mm, 5 whorls 1.8-2.26mm, 7 whorls 3.6-4 mm	3 whorls 1.4mm, 4 whorls 1.9-2.2 mm, 5 whorls 2.45mm	3 whorls 1.4-1.6 mm, 5 whorls 2.4-3 mm, 7 whorls 3.1-3.9 mm
Protoconch (µm)	240-415	320-410	390-470

Microspheric form (B-form)

Characters	*Assilina aspera*	*Assilina* ex. interc. *cuvillieri-tenuimarginata*
Diameter (mm) Thickness (mm)	8.1-8.3 2	11-17.8 1.6-3
Rate of spire opening	1 (second whorl), 1.1, 1.1, 1.6, 2, 2.2, 2.4, 3.2, 5, 5.4, 7.6	1 (second whorl), 1.5, 1.8, 3, 3, 3.2, 4.8, 5, 6.6, 6.6, 7.4, 8.4, 11, 11
Number of whorls per radius per mm	3 whorls 1.3 mm, 5 whorls 2.2-3 mm, 7 whorls 4.1-5.3 mm, 9 whorls 6.2-6.4	11 whorls 4.7-6.1 mm, 13 whorls 5.8-7.8, 15 whorls 7.1-8

whorls in a radius of 4.7-6.1 mm, 13 whorls in a radius of 5.8-7.8 mm, 15 whorls in a radius of 7.1-8 mm.

Remarks: This species differs from *A. exponens* in having smaller size of the test with thinner periphery. In addition, our specimens resemble *A. tenuimarginata* in having a similar test shape and external structure, as well as the proloculus diameter, but it differs from the latter in possessing small test and tighter whorls. There are close similarities between our specimens and original descriptions of the holotype and other types of *A. cuvillieri* (Schaub, 1981) in terms of the test size, external and internal structures. But our specimens occur in younger stratigraphic levels than the *A. cuvillieri s. str.* in the late Cuisian.

Assilina aspera Doncieux, 1948

Fig. 4a-j

1948. *Assilina aspera* Doncieux, p. 25, pl. 6, figs 15-25.
1976. *Assilina* aff. *aspera* (Doncieux).– Sirel & Gündüz, lev. XII, figs 6-13.
1981. *Assilina* aff. *tenuimarginta* (Heim).– Schaub, pl. 91. figs 10, 11, 14.
1982. *Assilina aspera* Doncieux.– Mojab, pl. 3.1, figs a-i.
2018. *Assilina aspera* Doncieux.– Sirel & Deveciler, p. 181, pl. 50, figs 1-8.

Number of specimens examined: 9

Description: The megalospheric generation has a biumbonate lenticular form and rounded margin with a diameter of 6.7-7.7 mm and thickness of 1.8-2 mm (Tabl. 1). The central umbo is filled by closely packed large granules whilst they are weakly scattered on the spiral patterns in middle-outer portions of concentric circles and between straight septal filaments. The height of the central part with a conspicuous concentration of granules is 1/3 to 1/2 of the radius of the test whereas the diameter of one is almost equal. The steps of spire openings are with an increase gradually from the first to last whorl, which is accompanied by isometric chambers, sometimes subrectangular and higher than long in middle-outer whorls. The septa are straight and become

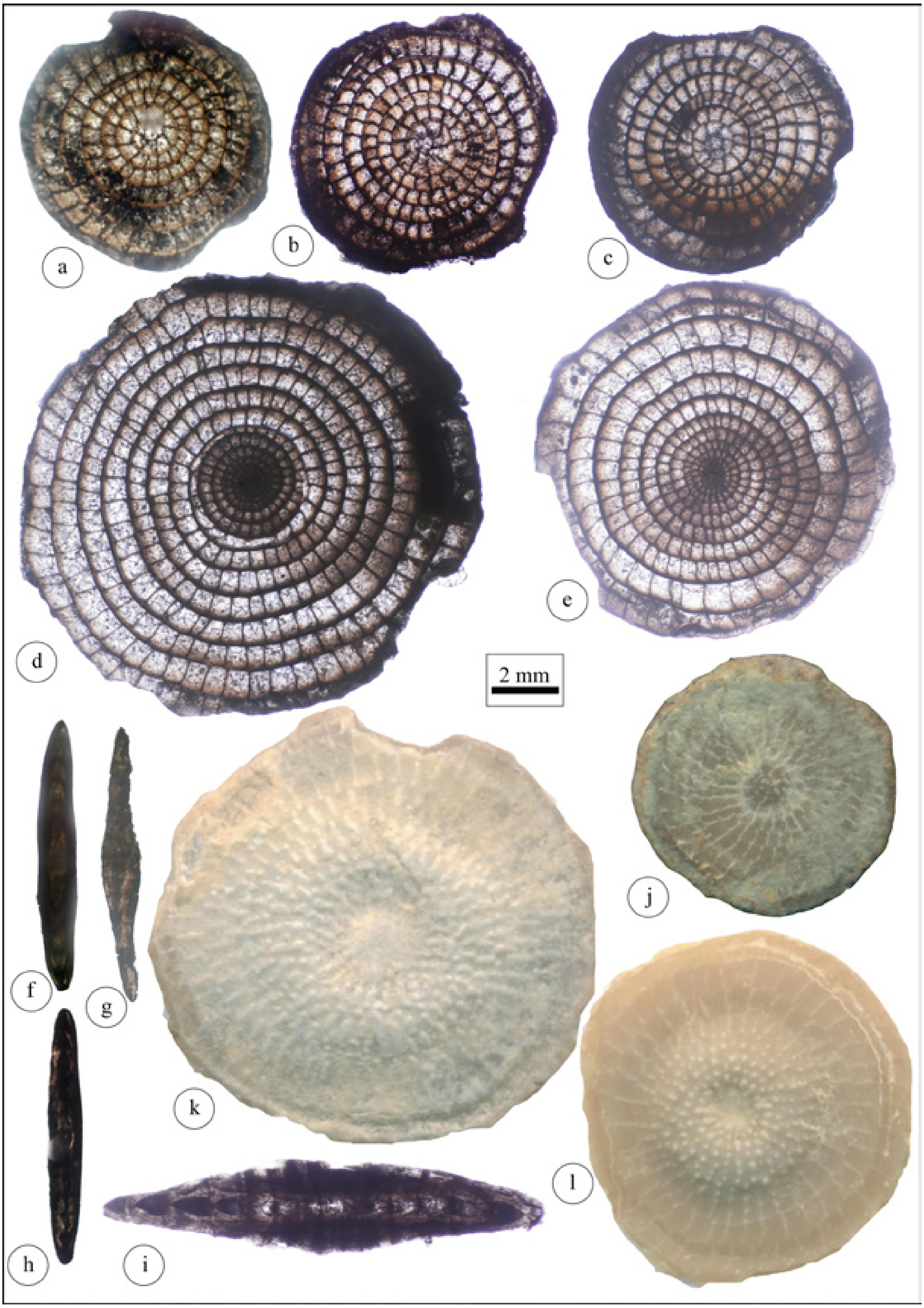

Fig. 2: **(a-l)** Equatorial and axial sections of both megalospheric and microspheric form of *Assilina* ex. interc. *cuvillieri-tenuimarginata*: **(a-c, f-h, j)** megalospheric form, sample number: BD4-6, BD12-14: (a) sample BD4, (b) sample BD13, (c) sample BD6, (f) sample BD12, (g) sample BD5, (h) sample BD14. **(a-c)** equatorial sections, **(f-h)** axial sections, **(j)** external view. **(d-e, i, k-l)** microspheric form, sample number: BD9-11: (d) sample BD10, (e) sample BD11, (i) sample BD9. **(d-e)** equatorial sections, **(i)** axial section, **(k-l)** external views.

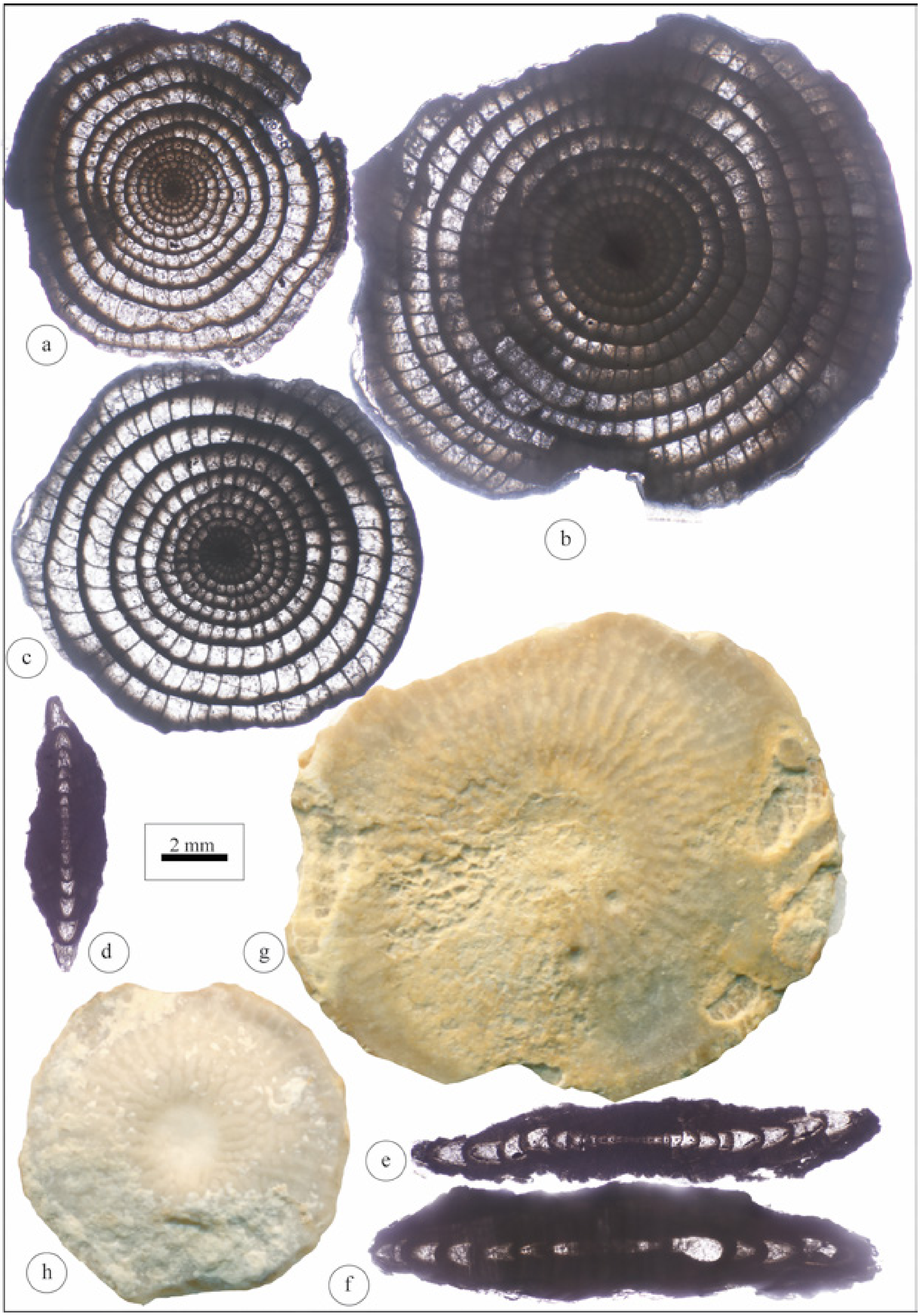

Fig. 3: **(a-h)** Equatorial and axial sections of microspheric form of *Assilina* ex. interc. *cuvillieri-tenuimarginata*: **(a-h)** megalospheric form, sample number: BD15-17, BD20-22: (a) sample BD15, (b) sample BD16, (c) sample BD17, (d) sample BD22, (e) sample BD21, (f) sample BD20. **(a-c)** equatorial sections, **(d-f)** axial sections, **(g-h)** external views.

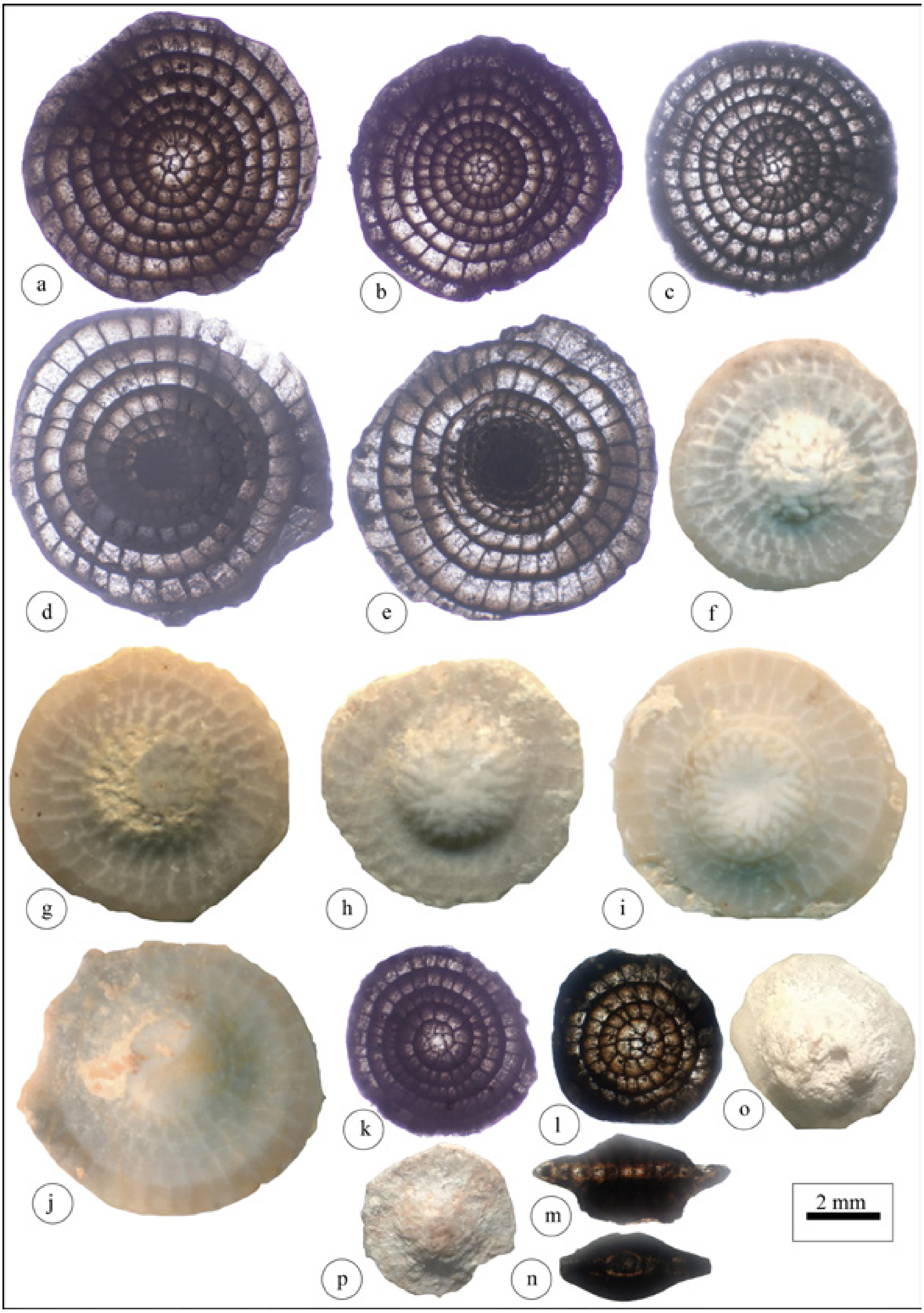

Fig. 4: **(a-j)** Equatorial sections of both megalospheric and microspheric form of *Assilina aspera*: **(a-c, f-h)** megalospheric form, sample number: BD26-28: (a) sample BD26, (b) sample BD27, (c) sample BD28. **(a-c)** equatorial sections. **(f-h)** axial sections. **(d-e, i-j)** microspheric form, sample number: BD29-30: (d) sample BD29, (e) sample BD30. **(d-e)** equatorial sections. **(i-j)** external views. **(k-p)** Equatorial and axial sections of both megalospheric form of *Assilina* aff. *aspera*: **(k-p)** megalospheric form, sample number: BD18-19, BD1-2: (k) sample BD18, (l) sample BD19, (m) sample BD1, (n) sample BD2. **(k-l)** equatorial sections, **(m-n)** axial sections, **(o-p)** external views.

slightly inclined in the outer portions. The marginal cord is relative thick through the whole whorls of the test. Number of whorls per radius is: 3 whorls in a radius of 1-1.26 mm, 5 whorls in a radius of 1.8-2.26 mm, and 7 whorls in a radius of 3.6-4 mm. The proloculus has diameter ranging from 240-415 µm (Tabl. 1).
The microspheric generation has a small-sized with morphological characters and structural elements on the test surface similar to those in the A-forms. The diameter ranges from 8.1 to 8.3 mm and thickness of 2 mm. The rate of spire opening increase gradually from the first to the last whorl, but in the last two whorls the height of chambers suddenly increases than the previous ones. The chambers are isometric or rarely higher than long in the last whorls with relatively thick and regular marginal cord in the whole whorls of the test. Septa are straight and somewhat inclined in the whole whorls, and occasionally becoming slightly curved at the last two whorls. Number of whorls per radius: 3 whorls in a radius of 1.3 mm, 5 whorls in a radius of 1.8-2.2 mm, 7 whorls in a radius of 2.7-2.9 mm, 8 whorls in a radius of 3.3-4 mm, and 9 whorls in a radius of 4 mm.
Remarks: Our specimens are obviously comparable with the figures of Mojab (1982, pl. 3, figs a-c and g-i) based on both external and internal structures and somewhat resemble the A-forms of Sirel & Deveciler (2018, pl. 50, figs 1-4). However, this species has been figured as *A*. aff. *tenuimarginata* in the Schaub (1981, pl. 91, figs 10, 11, 14) of the early Lutetian.

***Assilina* aff. *aspera* (Doncieux, 1948)**
Figs 3k-p

1948. *Assilina aspera* Doncieux, p. 25, pl. 6, figs 15-25.
1981. *Assilina* aff. *tenuimarginta* (Heim).– Schaub, pl. 91, figs 12-13.
1982. *Assilina* aff. *aspera* (Doncieux).– Mojab, pl. 3.2, figs b, h, i.

Number of specimens examined: 7
Description: The megalospheric generation has a small-sized, lenticular with raised umbonal area. The diameter ranges from 4.7 mm to 5.1 mm, thickness ranges from 1.8 mm to 2.1 mm. The arrangement of granules on the surface is much more concentrated on the central umbo, whilst they are slightly scattered in the peripheral margin. The diameter boss region is almost equal to the radius of the test, even if sometimes becomes a bit more. The rate of spire opening is similar to that of the first five whorls of the *Assilina aspera*. The chambers are isometric in the whole whorls of the test. The septa are straight and slightly inclined, with thick marginal cord. Number of whorls per radius is: 3 whorls in a radius of 1.4 mm, 4 whorls in a radius of 1.9-2.2 mm, and 5 whorls in a radius of 2.45 mm. The proloculus has diameter ranging from 320-410 µm (Tabl. 1).
Remarks: This form differs from *A. aspera* in having small size with the umbonal area that shows a gradual decrease in height towards the periphery, where the septal filaments are not present. Moreover, Doncieux (1948) has not provided the indispensable equatorial sections with good preservation and essential descriptions on the internal characters from the paratypes of *A. aspera*.

3.2. Larger benthic foraminifera

The distribution range of the LBF is well-known from the peri-Mediterranean region and Europe (Western Tethys), consistent with shallow benthic zone (SBZ) after Serra-Kiel *et al.* (1998) and after some modifications by Less & Özcan (2012), whereas systematic study of LBF Eocene assemblages from Iran is still with several gaps in understanding. The age attribution of the LBF regional faunas in the present article is only based on the co-occurrence of *A*. ex. interc. *cuvillieri-tenuimarginata*, *A*. *aspera*, and *A*. aff. *aspera*, and is not easily comparable with the SBZ zones. On the other hand, according to Serra-Kiel *et al.* (1998), although the stratigraphic position of *A*. ex. interc. *cuvillieri-tenuimarginata* could be into SBZ12-SBZ13, the appearance of *A*. *aspera* and *A*. aff. *aspera* was not assigned to this unit as a result of the previous studies, such as Schaub (1981). However, the first occurrences of them were just reported by several authors (Doncieux, 1948; Mojab, 1982; Sirel & Deveciler, 2018) in different localities (e.g. Madagascar, Iran and Turkey) of westernmost Mediterranean and central-eastern Tethyan regions during the early Lutetian.

3.3. Calcareous nannofossil

The variety and abundance of calcareous nannofossils is moderate to good in the studied samples. Although the etching, dissolution, or calcite overgrowth processes could be observed on the large-sized species of the *Micrantholithus*, *Discoaster*, *Reticulofenestra* genera, all taxa were easily identifiable. The rare specimens of upper Cretaceous and Paleocene taxa are reworked into the nannofossil assemblage, such as *Micula decussata* Vekshina, 1959, *Retecapsa ficula* Stover, 1966, *Prediscosphaera cretacea* Arkhangelsky, 1912, *Cribrosphaerella ehrenbergii* Arkhangelsky, 1912, *Arkhangelskiella cymbiformis* Vekshina, 1959, *cruciplacolithus primus* Perch-Nielsen, 1977, *Cr. tenuis* Stradner, 1961, *Ellipsolithus macellus* (Bramlette & Sullivan, 1961, and *Discoaster multiradiatus* Bramlette & Riedel, 1954. Generally, *Coccolithus pelagicus* Wallich, 1877, *Reticulofenestra dictyoda* Deflandre, 1954, and *R. minuta* Roth, 1970, are the majority of species (about 70%), which are visible within the calcareous nannofossils assemblages of studied samples. Moreover, other species are as follows: *Blackites tenuis* Bramlette & Sullivan, 1961, *Clausicoccus norrisii* Bown

& Newsam, 2017, *Coccolithus foraminis* Bown, 2005, *Co. latus* Bown, 2005, *Co. pauxillus* Bown, 2010, *Co.* cf. *gigas* Bramlette & Sullivan, 1961, *Discoaster kuepperi* Stradner, 1959, *D. nodifer* Bramlette & Riedel, 1954, *D. saipanensis* Bramlette & Riedel, 1954, *D. sublodoensis* Bramlette & Sullivan, 1961, *Nannotetrina alata* Martini, 1960, *Micrantholithus disculus* Bramlette & Riedel, 1954, *M. flos* Deflandre, 1954, *M. minimus* Bown & Dunkley, 2006, *Sphenolithus perpendicularis* Shamrock, 2010, *S. editus* Perch-Nielsen, 1978, *S. radians* Deflandre, 1952, *S. spiniger* Bukry, 1971, *Toweius callosus* Perch-Nielsen, 1971, *T. pertusus* Sullivan, 1965, *Umbilicosphaera protoannulus* Gartner, 1971, and *Reticulofenestra wadeae* Bown, 2005. Although it seems that some above-mentioned species are reworked from older stratigraphic level than the Lutetian (e.g. Ypresian stage) into studied calcareous nannofossil assemblages, for example: *Co. foraminis*, *Co. latus, T. pertusus*, and *S. editus*. Images of stratigraphically important and common species are shown in Figures 5-7.

Previously, the first appearances (FAs) of *B. gladius* Locker, 1967, *Co. gigas* (= *Chiasmolithus gigas* Bramlette & Sullivan, 1961), *N. alata*, and *S. perpendicularis* have been used by different authors to define the NP15 biozone and/or the other time equivalent biozones in the Lutetian age (Tabl. 2). The FA of *Nannotetrina* genera (or the species of *N. fulgens* Stradner, 1960/*N. quadrata* Bukry, 1973) is introduced for detecting lower boundary of the NP15 zone (Martini, 1971; Perch-Nielsen, 1985), while the Varol (1989) and Agnini *et al.* (2014) had reported the species within the Zone of NP15. The FAs of *N. alata* and *B. gladius* have been employed to define the base of zones CNE9 and NNTe8B by Agnini *et al.* (2014) and Varol (1989), respectively (Fig. 8). It should be noted that the latter boundaries (base of CNE9 or NNTe8B) are correspondent to the lower boundary of the NP15 and CP13a biozones (Fig. 8). Moreover, the FA of *Co. gigas* is used to define the base of zones CP13b and CNE10 by Okada & Bukry (1980) and Agnini *et al.* (2014), respectively (Fig. 8). Based on the previous studies (Shamrock, 2010; Bown & Dunkley Jones, 2012; Agnini *et al.,* 2014), the first occurrence of *S. perpendicularis*, and the last presence of *D. sublodoensis* have been visible from the basal parts of Zone NP15.

Hence, the lower part of the NP15 zone and also the zones of CNE9-CNE10 are suggested for the studied interval of Jahrum Formation based on the above-mentioned descriptions, published standard biozonation schemes (e.g. Martini, 1971; Okada & Bukry, 1980; Varol, 1989; Agnini *et al.,* 2014), and also absence/non-appearance of the *S. cuniculus* Bown, 2005, *S. furcatolithoides* Locker, 1967, *D. bifax* Bukry, 1971, or *R. umbilicus* Levin, 1965 species, in the present study (Fig. 8). The zone of NP15 indicates the early Lutetian age and it can be equivalent to the CNE9-10 zones of Agnini *et al.* (2014), and the CP13a-b of Okada & Bukry (1980) in the low latitude sites, and also with the NNTe8B Zone of Varol (1989) in the mid to high latitude (Fig. 8).

Table 2: The detected calcareous nannofossil species from the studied interval of Jahrum Formation (at the Buldaji section), and their distribution ranges based on the Perch-Nielsen (1985).The highlighted row shows the identified calcareous nannofossil biozone.

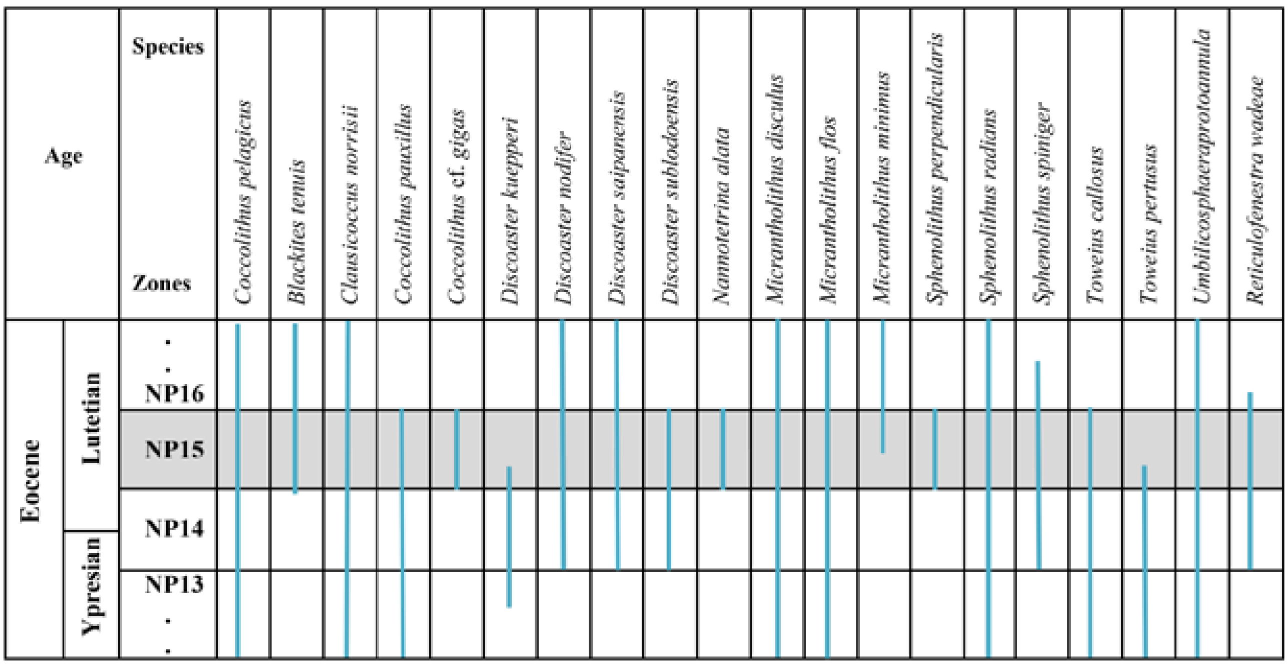

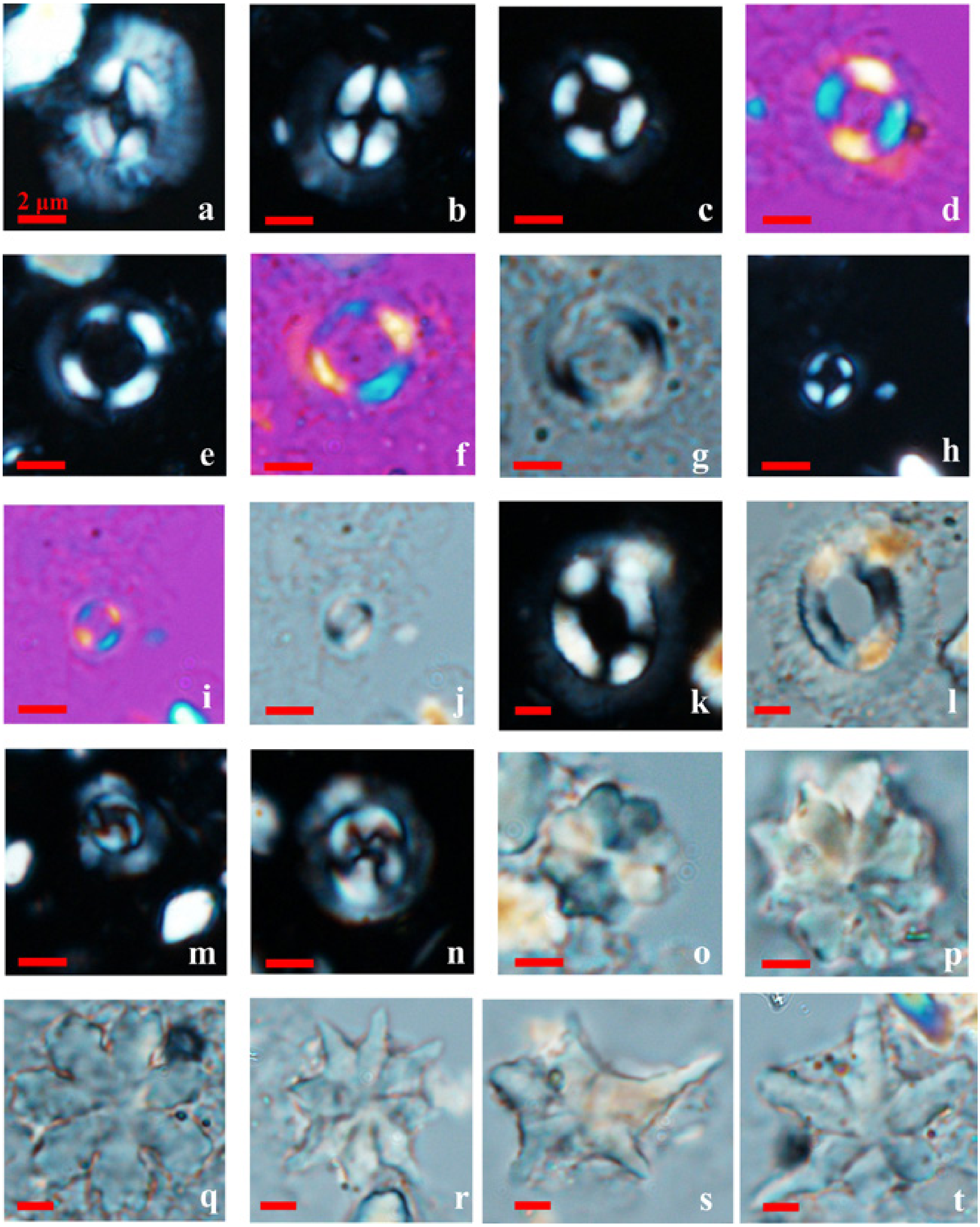

Fig. 5: **(a-b)** *Coccolithus pelagicus* (figs a & b: XPL), sample No. n2. **(c-d)** *Coccolithus foraminis* (fig. c: XPL, fig. d: GP), sample No. n7. **(e-g)** *Coccolithus latus* (fig. e: XPL, fig. f: GP, fig. g: QP), sample No. n6. **(h-j)** *Coccolithus pauxillus* (fig. h: XPL, fig. i: GP, fig, j: QP), sample No. n1. **(k-l)** *Coccolithus* sp. (fig. k: XPL, fig. l: QP), sample No. n2. **(m-n)** *Toweius pertusus* (figs m & n: XPL), sample No. n1. **(o-p)** *Discoaster kuepperi* (figs o & p: QP), sample No. n1. **(q)** *Discoaster nodifer* (fig. q: QP), sample No. n3. **(r)** *Discoaster saipanensis* (fig. r: QP), sample No. n4. **(s)** *Discoaster sublodoensis* (fig. s: QP), sample No. n2. **(t)** *Discoaster* cf. *sublodoensis* (fig. t: QP), sample No. n3. Scale bar is 2 µm for all pictures. XPL= Cross Polarizing Light; GP= Gypsum Plate; QP= Quartz Plate.

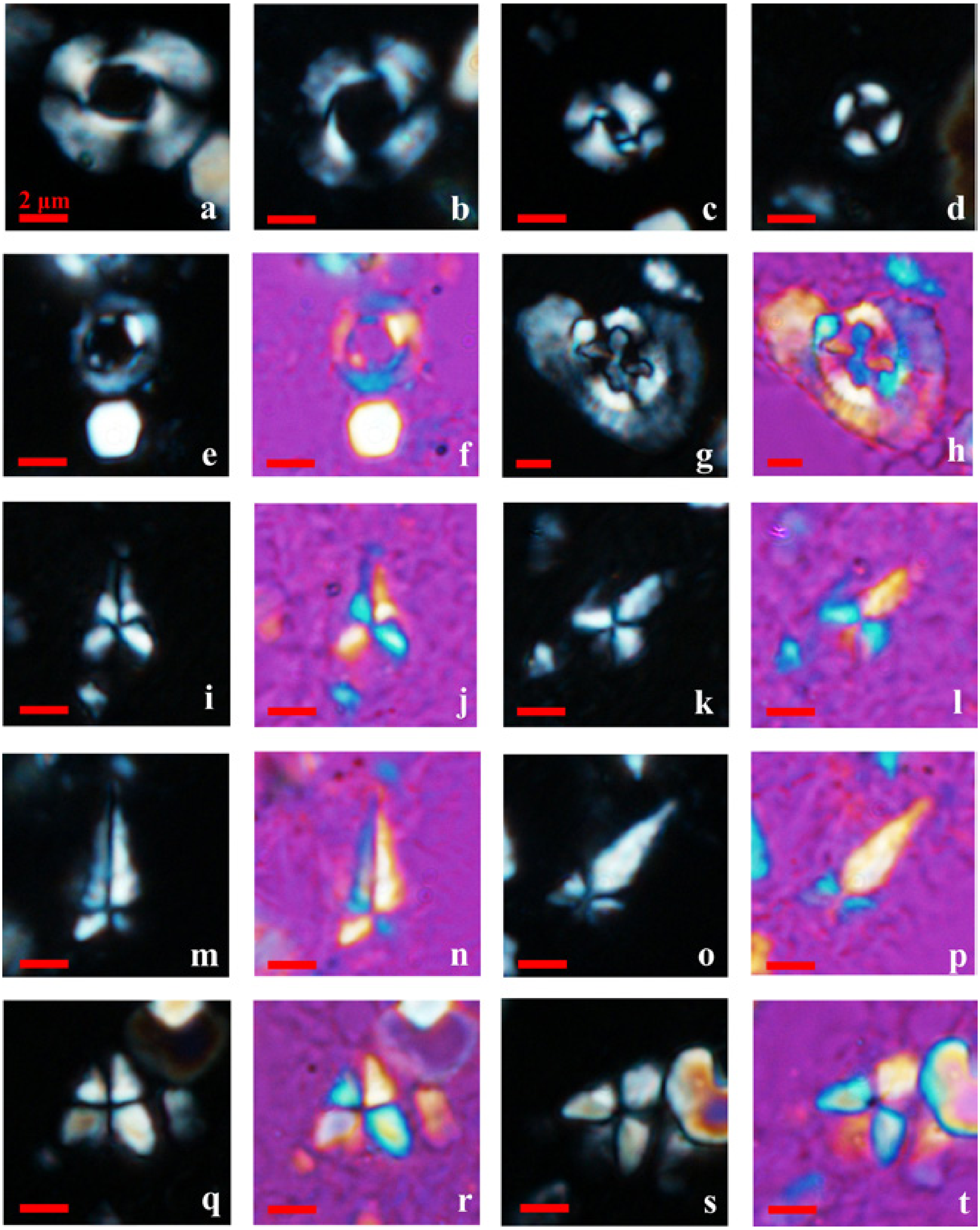

Fig. 6: **(a)** *Reticulofenestra dictyoda* (fig. a: XPL), sample No. n1. **(b)** *Reticulofenestra wadeae* (fig. b: XPL), sample No. n2. **(c)** *Reticulofenestra* sp. (fig. c: XPL), sample No. n2. **(d)** *Toweius callosus* (fig. d: XPL), sample No. n4. **(e-f)** *Umbilicosphaera protoannulus* (fig. e: XPL, fig. f: GP), sample No. n5. **(g-h)** *Coccolithus* cf. *gigas* (fig. g: XPL, fig. h: GP), sample No. n5. **(i-l)** *Sphenolithus editus* (figs. i & j: 0º, figs k & l: 45º, figs. i & k: XPL, figs j & l: GP), sample No. n7. **(m-p)** *Sphenolithus radians* (figs m & n: 0º, figs. o & p: 45º, figs m & o: XPL, figs n & p: GP), sample No. n4. **(q-t)** *Sphenolithus spiniger* (figs q & r: 0º, figs. s & t: 45º, figs q & s: XPL, figs r & t: GP), sample No. n5. Scale bar is 2 µm for all pictures. XPL= Cross Polarizing Light; GP= Gypsum Plate; QP= Quartz Plate.

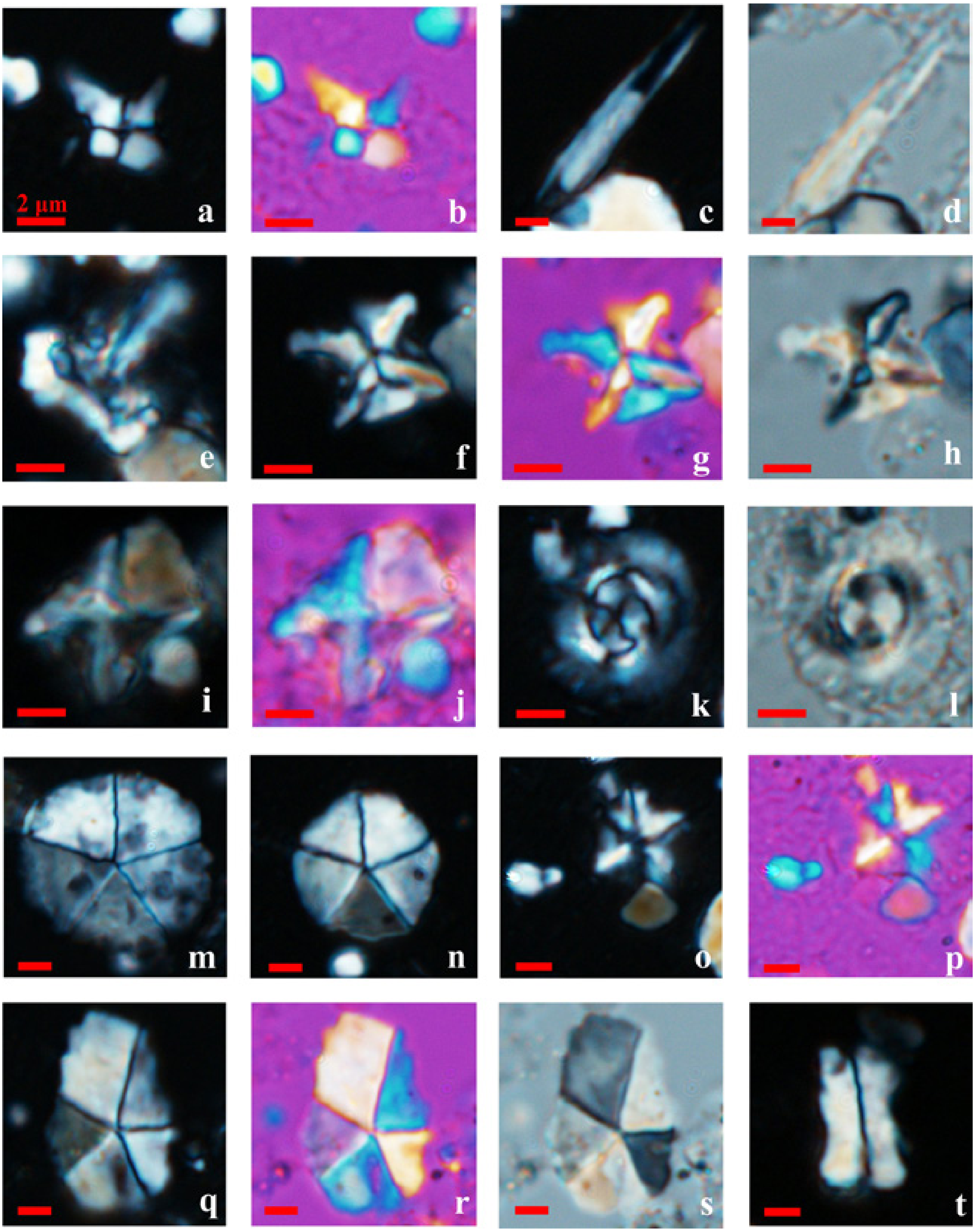

Fig. 7: **(a-b)** *Sphenolithus perpendicularis* (fig. a: XPL, fig. b: GP), sample No. n1. **(c-d)** *Blackites tenuis* (figs c & d: 45º, fig. c: XPL, fig. d: QP), sample No. n1. **(e)** *Prediscosphaera* sp. (fig. e: 45º, XPL), sample No. n1. **(f-h)** *Nannotetrina alata* (fig. f: XPL, fig. g: GP, fig. h: QP), sample No. n1. **(i-j)** *Nannotetrina alata* (fig. i: XPL, fig. j: GP), sample No. n2. **(k- l)** *Clausicoccus norrisii* (fig. k: XPL, fig. l: QP), sample No. n6. **(m)** *Micrantholithus disculus* (fig. m: XPL), sample No. n4. **(n)** *Micrantholithus flos* (fig. n: XPL), sample No. n6. **(o-p)** *Micrantholithus minimus* (fig. o: XPL, fig. p: GP), sample No. n8. **(q-s)** *Micrantholithus* sp. (fig. q: XPL, fig. r: GP, fig. s: QP), sample No. n8. **(t)** *Zygrhablithus bijugatus* (fig. t: XPL), sample No. n7. Scale bar is 2 µm for all pictures. XPL= Cross Polarizing Light; GP= Gypsum Plate; QP= Quartz Plate.

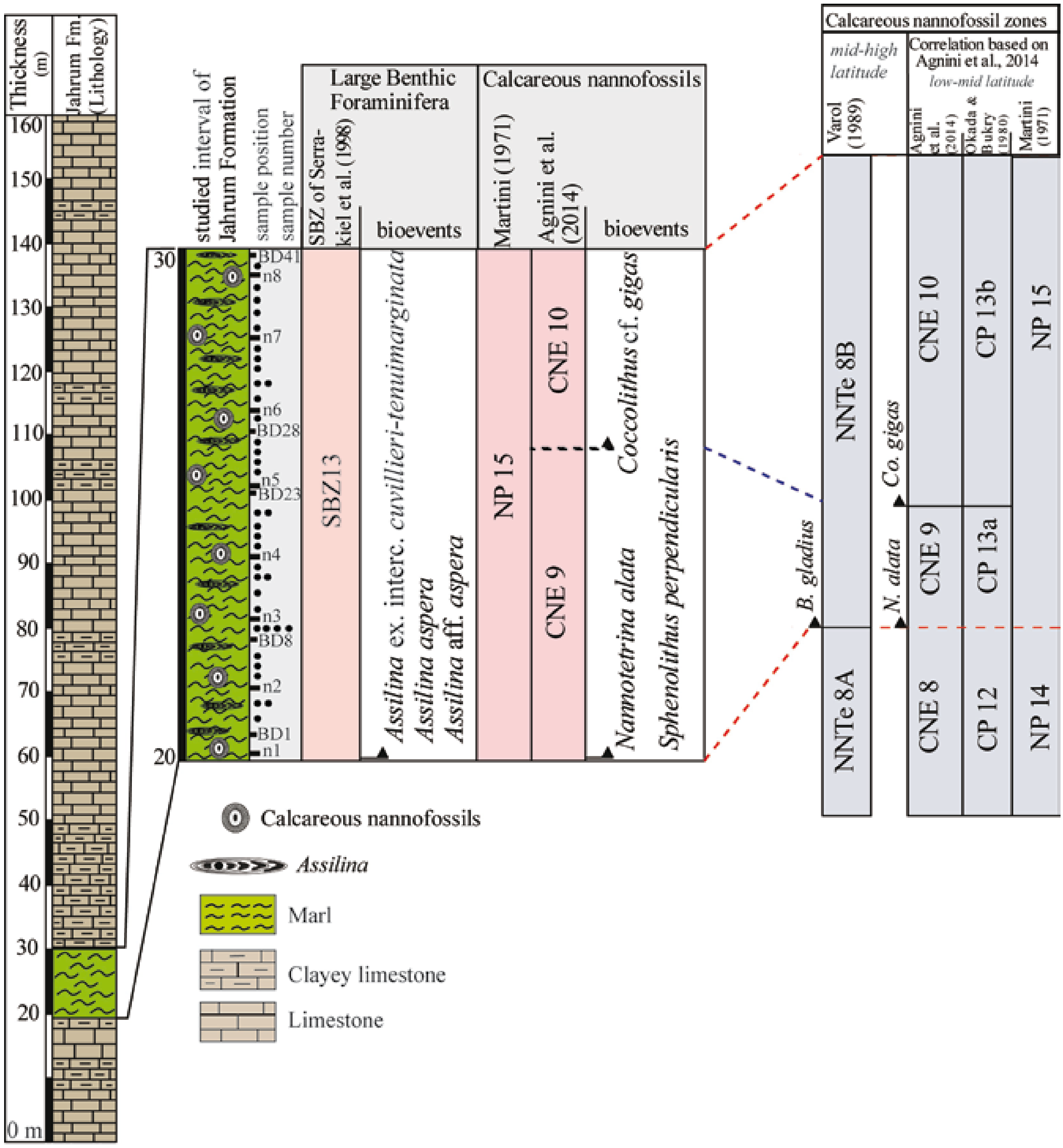

Fig. 8: Stratigraphic log of the Buldaji section show the correlation between LBF and calcareous nannofossils biozones. The studied biozones are compared with Agnini *et al.* (2014) and Varol (1989) studies. Note that the arrows are only used to display the appearance of the species into the marly interval.

4. CONCLUSIONS

For the first time, the detailed taxonomical study of the early Lutetian *Assilina* species found in Jahrum Formation has allowed us to identify three species (*A*. ex. interc. *cuvillieri-tenuimarginata*, *A*. *aspera,* and *A*. aff. *aspera*). Our finding on the genus *Assilina* is relatively reliable for age determination and correlation of them with SBZ zones of the western Tethys in the studied interval. Nevertheless, there is independent evidence of nannofossil data that could provide an accurate age for the *Assilina* assemblages. The result of calcareous nannofossil studies with a moderate diversity and abundance and occurrences of index zonal markers such as *Co*. cf. *gigas*, *N. alata*, *S. perpendicularis* are indicative of lower parts of the NP15 Zone of Martini (1971) (and also the CNE9-CNE 10 zones of Agnini *et al.* (2014), that suggest the exact age of the *Assilina* assemblages, *A*. ex. interc. *cuvillieri-tenuimarginata*, *A*. *aspera*, and *A*. aff. *aspera,* into the upper part of the SBZ13 (Fig. 8). In addition, the simultaneous occurrence of the *A*. ex. interc. *cuvillieri-tenuimarginata*, *A*. *aspera*, and *A*. aff. *aspera* were recorded for the first time in accordance with the biostratigraphical age of SBZ13 from all over the Tethyan ocean.

ACKNOWLEDGEMENTS

We would like to thank O. Varol (Varol research company, USA) for his advice and checking of calcareous nannofossils determinations. MP is grateful to National Iranian Oil Company for providing the opportunity of this study. MMA appreciate field and laboratory support by E. Khosravi and M. Fallah. We are grateful to E. Özcan (Istanbul Technical University), and an anonymous reviewer, as well as associate editor A. Piuz who helped a lot in improving the manuscript. Special thanks due to S. Sarkar (University of Bristol) for linguistic improvements.

REFERENCES

Agnini C., Fornaciari E., Raffi I., Catanzariti R., Pälike H., Backman J. & Rio D. 2014. Biozonation and biochronology of Paleogene calcareous nannofossils from low and middle latitudes. *Newsletters on Stratigraphy*, 47(2): 131-181.

Ahmad S., Jalal W., Ali F., Hanif M., Ullah Z., Khan S., Ali A., Jan I.U. & Rehman K. 2015. Using larger benthic foraminifera for the paleogeographic reconstruction of Neo-Tethys during Paleogene. *Arabian Journal of Geoscience*, 8: 5095-5110.

Ala M.A. 1982. Chronology of trap formation and migration of hydrocarbons in Zagros sector of southwest Iran. *AAPG Bulletin*, 66(10): 1535-1541.

Alavi M. 1991. Sedimentary and structural characteristics of the Paleo-Tethys remnants in northeastern Iran. *American Journal of Science*, 304: 1-20.

Alavi M. 2004. Regional stratigraphy of the Zagros fold-thrust belt of Iran and its proforeland evolution. *Geological Society of America Bulletin*, 103(8): 983-992.

Almasinia B. 2017. Microfacies, biostratigraphy and sedimentary environments of the Eocene sedimentary successions in the Zagros and Sanandaj-Sirjan Zone (Iran) (Doctoral dissertation, Friedrich-Alexander-Universität Erlangen-Nürnberg [FAU]).

Amirshahkarami M. & Zebarjadi E. 2018. Late Paleocene to Early Eocene larger benthic foraminifera biozones and microfacies in Estahbanate area, Southwest of Iran with Tethyan biozones correlation. *Carbonates and Evaporites*, 33(4): 869-884.

Aubry M.P. 1984. *Handbook of Cenozoic calcareous nannoplankton*. Book 1: Ortholithae (Discoasters). Micropaleontology Press, American Museum of Natural History, New York, 265 pp.

Aubry M.P. 1989. *Handbook of Cenozoic calcareous nannoplankton*. Book 3: Ortholithae (Pentaliths, and others) Heliolithae (Fasciculiths, Sphenoliths and others). Micropaleontology Press, American Museum of Natural History, New York, 279 pp.

Bahroudi A. & Koyi H.A. 2004. Tectono-sedimentary framework of the Gachsaran Formation in the Zagros foreland basin. *Marine and Petroleum Geology*, 21(10): 1295-1310.

Ben İsmail-Lattrache K., Özcan E., Boukhalfa K., Saraswati P.K., Soussi M. & Jovane L. 2014. Early Bartonian orthophragminids (Foraminiferida) from Reineche Limestone, north African platform, Tunisia: taxonomy and paleobiogeographic implications. *Geodinamica Acta*, 26: 94-121.

Berggren W.A. & Pearson P.N. 2005. A revised tropical to subtropical Paleogene planktonic foraminiferal zonation. *The Journal of Foraminiferal Research*, 35(4): 279-298.

Berggren W.A., Kent D.V., Swisher C.C. & Aubry M.P. 1995. A revised Cenozoic geochronology and chronostratigraphy. *In*: Berggren W.A., Kent D.V., Aubry M.P. & Hardenbol J. (Eds), *Geochronology - Time Scales and Global Stratigraphic Correlation*. Special Publications-SEPM, 54: 129-212.

Boukhary M. 1988. *Nummulites bullatus* Azzaroli, 1952, from Egypt and its biostratigraphic significance. *Neues Jahrbuch für Geologie und Paläontologie,* Abhandlungen, 177: 243-262.

Boukhary M., Bassiouni M. A. & Kamal Y. 1995. *Nummulites luterbacheri* n. sp., unexpected large Nummulites from basal Ilerdian (Early Eocene) from El Quss Abu Said, Farafra Oasis, Western Desert, Egypt. *Revue de Micropaléontologie,* 38(4): 285-298.

Bown P.R. 2005. Palaeogene calcareous nannofossils from the Kilwa and Lindi areas of coastal Tanzania (Tanzania Drilling Project 2003-4). *Journal of Nannoplankton Research*, 27: 21-95.

Bown P.R. & Dunkley Jones T. 2012. Calcareous nannofossils from the Paleogene equatorial Pacific (IODP Expedition 320 Sites U1331-1334). *Journal of Nannoplankton Research*, 32: 3-51.

Bown P. & Young J. 1998. Techniques. *In*: Bown P.R. (Ed), *Calcareous Nannofossil Biostratigraphy*. Chapman & Hall, Cambridge: 16-28.

Deveciler A. 2014. Description of Larger Benthic Foraminifera

Species from the Bartonian of Yakacık Memlik Region (N Ankara, Central Turkey). *Bulletin of the Earth Sciences Application and Research Centre of Hacettepe University*, 35(2): 137-150.

Doncieux L. 1948. Les Foraminiferes Eocènes et Oligocènes de l'ouest de Madagascar. *Annales géologiques du service des mines*, 13: 8-33.

Farinacci A. & Howe R. 2016. Catalog of Calcareous Nannofossils, expansion and renaming. Nannotax website (www.mikrotax.org).

Hadi M. & Vahidinia M. 2019. Biostratigraphy of larger benthic foraminifera from Cuisian and Bartonian limestones from the Torbat-e-Heydarieh region (Central Iran). *Neues Jahrbuch für Geologie und Paläontologie, Abhandlungen*, 291(3): 299-315.

Hadi M., Vahidinia M. & Juraj H. 2019a. Larger foraminiferal biostratigraphy and microfacies analysis from the Ypresian (Ilerdian-Cuisian) limestones in the Sistan Suture Zone (eastern Iran). *Turkish Journal of Earth Sciences*, 28: 122-145.

Hadi M., Vahidinia M. & Abbassi N. 2019b. Ilerdian-Cuisian Alveolinids from the western Alborz and eastern Iran zones: systematic and biostratigrapic implications. *Journal of Foraminiferal Research*, 49(2): 141-162.

Hadi M., Less G. & Vahidinia M. 2019c. Eocene larger benthic foraminifera (alveolinids, nummulitids, and orthophragmines) from the eastern Alborz region (NE Iran): taxonomy and biostratigraphy implications. *Revue de Micropaléontologie*, 63(2): 65-84.

Heim A. 1908. Die Nummuliten und Flyschbildungen des Schweizeralpen. *Abhandlungen der Schweizerischen Paläontologischen Gesellschaft*, 35: 1-301.

Heydari E. 2008. *Tectonics* versus eustatic control on supersequences of the Zagros Mountains of Iran. *Tectonophysics*, 451(1-4): 56-70.

Hottinger L. 2007. Revision of the foraminiferal genus *Globoreticulina* Rahaghi, 1978, and of its associated fauna of larger foraminifera from the late Middle Eocene of Iran. *Carnets de Géologie/Notebooks on Geology*, 6: 1-51.

Izadighalati S. & Ahmadi V. 2017. Microbiostratigraphy of the Upper Paleocene to Middle Eocene Jahrum Formation in the Folded Zagros Zone, SW Iran. *Stratigraphy and Geological Correlation*, 25(7): 759-770.

James G.A. & Wynd J.G. 1965. Stratigraphic nomenclature of Iranian oil consortium agreement area. *AApG Bulletin,* 49(12): 2182-2245.

Kahtibi-Mehr M., Adabi M., Tasouj M.M., Vaziri-Moghaddam H. & Sadeghi A. 2012. Depositional environment, geochemistry and sequence stratigraphy of the Jahrum Formation in Buldaji Area, Zagros basin. *Journal of Researches in Earth Sciences*, 11(3): 85-103 (in Persian).

Less G. & Özcan E. 2012. Bartonian-Priabonian larger benthic foraminiferal events in the Western Tethys. *Austrian Journal of Earth Sciences*, 105: 129-140.

Martini E. 1971. Standard Tertiary and Quaternary calcareous nannoplankton zonation. *In*: Farinacci A. (Ed), *Proceedings II Planktonic Conference*, Roma 1970, 2: 739-785.

Maghfouri-Moghadam I. & Taherpour Khalil-Abad M. 2012. Microbiostratigraphy of Middle Eocene Shahbazan Formation at the southeastern flank of Chenar Anticline, Lurestan Basin, Sw Iran. *Iranian Journal of Earth Sciences*, 5: 74-81.

Mojab F. 1982. Middle Eocene assilinid foraminifera from Iran. *In:* Banner F.T. & Lord A.R. (eds), *Aspects of Micropalaeontology.* Springer, Dordrecht, pp. 81-110.

Motiei H. 1993. *Stratigraphy of Zagros*. Treatise on the Geology of Iran, Tehran, 151 pp.

Okada H. & Bukry D. 1980. Supplementary modification and introduction of code numbers to the low-latitude coccolith biostratigraphic zonation (Bukry, 1973; 1975). *Marine Micropaleontology*, 5: 321-325.

Özcan E., Hanif M., Ali N. & Yücel A.O. 2015. Early Eocene orthophragminids (Foraminifera) from the type-locality of *Discocyclina ranikotensis* Davies, 1927, Thal, NW Himalayas, Pakistan: insights into the orthophragminid palaeobiogeography. *Geodinamica Acta*, 27: 267-299.

Özcan E., Ali N., Hanif M., Hashmi S.I., Khan A., Yücel A.O. & Abbasi İ.A. 2016. A New Priabonian Heterostegina from the eastern Tethys (Sulaiman fold belt, west Pakistan): implications for the development of eastern Tethyan Heterostegines. *Journal of Foraminifera Research*, 46: 393-408.

Özcan E., Pignatti J., Pereira C., Yücel A. O., Drobne K., Barattolo F. & Saraswati P.K. 2018. Paleocene orthophragminids from the Lakadong Limestone, Mawmluh Quarry section, Meghalaya (Shillong, NE India): implications for the regional geology and paleobiogeography. *Journal of Micropalaeontology*, 37(1): 357-381.

Parandavar M. & Hadavi F. 2019. Identification of the Oligocene-Miocene boundary in the Central Iran Basin (Qom Formation): Calcareous nannofossil evidences. *Geological Quarterly*, 63(2): 215-229, doi: 10.7306/gq.1464.

Pavlovec R. 2003. Nummulitids from flysch in surroundings of Ilirska Bistrica, southwest Slovenia. *Geologija*, 46(2): 1-244.

Perch-Nielsen K. 1985. Cenozoic calcareous nannofossils. *In*: Bolli H.M., Saunders J.B. & Perch-Nielsen K. (Eds), *Plankton Stratigraphy 1*. Cambridge University Press, Cambridge: 427-554.

Rahaghi A. 1978. *Paleogene biostratigraphy of some parts of Iran*. Tehran, National Iranian Oil Company, Geological Laboratories, 164 pp.

Rahaghi A. 1980. *Tertiary faunal assemblage of Qum-Kashan, Sabzewar and Jahrum areas*. Tehran, National Iranian Oil Company, Geological Laboratories, 64 pp.

Rahaghi A. & Schaub H. 1976. Nummulites et Assilines du NE de l'Iran. *Eclogae Geologicae Helvetiae*, 69: 765-782.

Romein A.J.T. 1979. *Lineages in early Paleogene calcareous nannoplankton.* Doctoral dissertation, Utrecht University.

Schaub H. 1981. Nummulites et Assilines de la Téthys paléogène: Taxinomie, phylogenèse et biostratigraphie. *Schweizerische paläontologische Abhandlungen,* 104/106, 236 pp.

Serra-Kiel J., Hottinger L., Caus E., Drobne K., Ferrandez C., Jauhri A.K., Less G., Pavlovec R., Pignatti J. & Samso J.M. 1998. Larger foraminiferal biostratigraphy of the Tethyan Paleocene and Eocene. *Bulletin de la Société géologique de France*, 169: 281-299.

Shafaii Moghadam H. & Stern R.J. 2014. Ophiolites of Iran: Keys to understanding the tectonic evolution of SW Asia: (I) Paleozoic ophiolites. *Journal of Asian Earth Sciences*, 91: 19-38.

Shamrock J.L. 2010. *Eocene calcareous nannofossil biostratigraphy, paleoecology and biochronology of ODP leg 122 hole 762c, Eastern Indian Ocean (exmouth plateau).*

University of Nebraska-Lincoln Follow, PhD thesis, 160 pp.

Sherkati S. & Letouzey J. 2004. Variation of structural style and basin evolution in the central Zagros (Izeh zone and Dezful Embayment), Iran. *Marine and petroleum geology*, 21(5): 535-554.

Stöcklin J. 1968. Structural history and tectonics of Iran: A review. *AAPG Bulletin*, 52: 1229-1258.

Sirel E. & Deveciler A. 2018. *Description and Some Revision of Ranikothalia Caudri, Nummulites Lamarck and Assilina D'Orbigny Species From Thanetian-Early Chattian of Turkey*. Ankara Üniversite Yayınevi, 131 pp.

Sirel E. & Gündüz H. 1976. Haymana (G Ankara) yöresi İlerdiyen, Küiziyen ve Lütesiyen' deki Nummulites, Assilina ve Alveolina cinslerinin bazı türlerinin tanımlamaları ve stratigrafik dağılımları. *Türkiye Jeoloji Kurumu Bülteni*, 19: 31-44.

Varol O. 1989. Eocene calcareous nannofossils from Sile (Northwest Turkey). *Revista Española de micropaleontología*, 21: 273-320.

Vaziri-Moghaddam H., Seyrafian A. & Taraneh P. 2002. Biofacies and sequence stratigraphy of the Eocene succession, at Hamzeh-Ali area, north-central Zagros, Iran. *Carbonates and Evaporites*, 17(1): 60-67.

Zhang Q., Willems H. & Ding L. 2013. Evolution of the Paleocene-Early Eocene larger benthic foraminifera in the Tethyan Himalaya of Tibet, China. *International Journal of Earth Sciences*, 102: 1427-1445.